Photon-photon scattering, pion polarizability, and chiral symmetry

John F. Donoghue and Barry R. Holstein

Department of Physics and Astronomy, University of Massachusetts, Amherst, Massachusetts 01003

(Received 8 February 1993)

Recent attempts to detect the pion polarizability via analysis of $\gamma\gamma \to \pi\pi$ measurements are examined. The connection between calculations based on dispersion relations and on chiral perturbation theory is established by matching the low-energy chiral amplitude with that given by a full dispersive treatment. Using the values for the polarizability required by chiral symmetry, predicted and experimental cross sections are shown to be in agreement.

I. INTRODUCTION

The reactions $\gamma\gamma \to \pi^0\pi^0$ and $\gamma\gamma \to \pi^+\pi^-$ represent currently interesting theoretical and experimental laboratories for chiral perturbation theory (χPT) [1] and for dispersion relations [2]. For charged pion production the χPT prediction is in good agreement with the data, as shown in Fig. 1 [3,4]. However, in the case of neutral pion production, the one-loop chiral perturbation theory calculation [4,5] disagrees even near threshold, with both a dispersive treatment and the data, as can be seen in Fig. 2 [6].[1] This situation at first appears surprising, as a dispersive calculation should obey the chiral strictures at low energy, while a chiral calculation should obey the unitarity properties to the order in energy that one is working. Of course, the chiral result is known to be an expansion in the energy, and it is always possible for higher orders to modify the first-order result [8]. However, in most other calculations the modifications are not very large near threshold. One of the purposes of this paper is to resolve the theoretical issue of the connection between the chiral and dispersive methods, and to understand the origin of large corrections to the $\gamma\gamma \to \pi^0\pi^0$ amplitude near threshold. We do this in Sec. II by matching the two descriptions, and providing an analytic solution to the dispersion relation which is consistent with the low-energy chiral properties. This exercise indicates that the two descriptions are in fact completely consistent in their respective limits, and suggests that rescattering effects required by unitarity are the dominant source of corrections to the lowest-order chiral prediction.

In addition, the two-photon reactions have been utilized phenomenologically in order to extract the pion electromagnetic polarizability [9]. For this purpose, one needs as accurate a description of the amplitude as possible, and we use our results from Sec. II to construct an improved picture of the transition amplitude in Sec. III. The connection with the polarizability and a review of the present experimental status is given in Sec. IV, and our results are summarized in Sec. V.

II. MATCHING THE CHIRAL AND DISPERSIVE DESCRIPTIONS

In this section our main interest is to understand how a dispersive treatment matches on to the calculation of chiral perturbation theory and to learn why there exist large corrections to the chiral results even near threshold. In a recent paper, Pennington has run a series of numerical exercises which suggest that the necessary modifications come from multiloop effects, which are of higher order in the chiral expansion [10]. Our analytic study, discussed
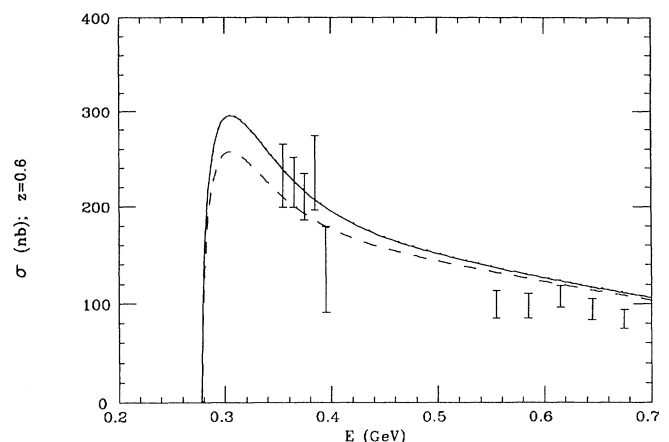

FIG. 1. The data points shown are the $\gamma\gamma \to \pi^+\pi^-$ cross section (with $|\cos\theta| < Z \equiv 0.6$) measured by the Mark II collaboration (Ref. [3]). The dashed curve is the Born approximation prediction, while the solid line is that from one-loop chiral perturbation theory.

---

[1] The dispersive prediction shown therein is that which we describe later in this paper, but it is similar to the pioneering dispersive calculation performed by Morgan and Pennington [7].
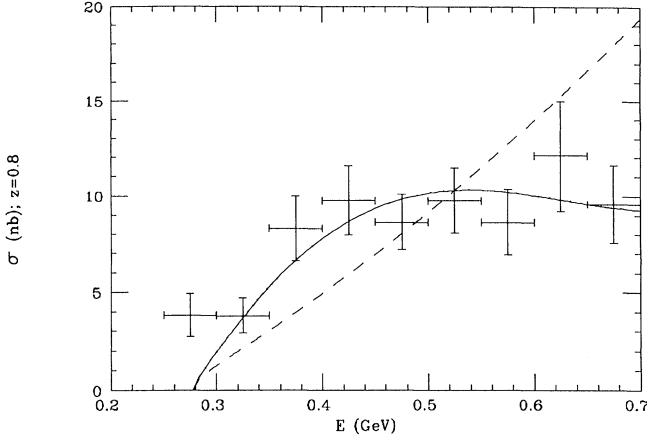
<u>48</u>   137

FIG. 2. The data points shown are the $\gamma\gamma \to \pi^0\pi^0$ cross section (with $|\cos\theta| < Z \equiv 0.8$) measured by the Crystal Ball Collaboration (Ref. [4]). The dashed curve is the prediction of one-loop chiral perturbation theory, while the solid curve is a full no-free-parameter dispersive calculation, as described in the text.

below, confirms this conclusion. In fact the results turn out to be quite simple, and we will be able to neatly identify the source of the corrections.

We begin by setting up a bit of formalism. We shall assume, consistent with the chiral expansion, that when we are in the near-threshold region the only relevant higher-order effects are in the helicity-conserving S-wave amplitude, which we write as

$$\gamma\gamma \to \pi^+\pi^- : \qquad f^C(s) = \frac{1}{3}\left[2f_0(s) + f_2(s)\right],$$

$$\gamma\gamma \to \pi^0\pi^0 : \qquad f^N(s) = \frac{2}{3}\left[f_0(s) - f_2(s)\right], \tag{1}$$

where $I = 0, 2$ refers to the isospin of the final $\pi\pi$ state. For neutral pion production and working in the gauge wherein $\epsilon_2 \cdot k_2 = \epsilon_2 \cdot k_1 = \epsilon_1 \cdot k_2 = \epsilon_1 \cdot k_1 = 0$ the transition amplitude is

$$\gamma\gamma \to \pi^0\pi^0 : \qquad \text{Amp} = 2ie^2\epsilon_1 \cdot \epsilon_2 f^N(s) \tag{2}$$

and the cross section is given by

$$\frac{d\sigma^N}{d\Omega} = \frac{\alpha^2}{4s}\beta(s)|f^N(s)|^2, \tag{3}$$

where

$$\beta(s) = \sqrt{\frac{s - 4m_\pi^2}{s}} \tag{4}$$

is the center of mass velocity of the produced pions. For convenience in comparison with experimental results it is useful to present also the total cross section for events having $|\cos\theta|$ less than some fixed value Z:

$$\sigma^N(|\cos\theta| < Z) = \frac{\pi\alpha^2 Z}{s}\beta(s)|f^N(s)|^2. \tag{5}$$

In the charged pion case the Born and Seagull contributions to this multipole must also be included, so that the full amplitude becomes

$$\gamma\gamma \to \pi^+\pi^- :$$

$$\text{Amp} = 2ie^2\left[\epsilon_1 \cdot \epsilon_2 a(s) - \frac{\epsilon_1 \cdot p_+\epsilon_2 \cdot p_-}{p_+ \cdot k_1} - \frac{\epsilon_1 \cdot p_-\epsilon_2 \cdot p_+}{p_+ \cdot k_2}\right] \tag{6}$$

with cross section

$$\frac{d\sigma^C}{d\Omega} = \frac{\alpha^2}{2s}\beta(s)\left[|a(s)|^2 - 2\,\text{Re}a(s)\frac{\beta^2(s)\sin^2\theta}{1 - \beta^2(s)\cos^2\theta}\right.$$
$$\left. + 2\frac{\beta^4(s)\sin^4\theta}{[1 - \beta^2(s)\cos^2\theta]^2}\right]. \tag{7}$$

Here

$$a(s) = 1 + f^C(s) - f^C_{\text{Born}}(s), \tag{8}$$

where

$$f^C_{\text{Born}}(s) = \frac{1 - \beta^2(s)}{2\beta(s)}\ln\left(\frac{1 + \beta(s)}{1 - \beta(s)}\right)$$
$$= f_0^{\text{Born}}(s) = f_2^{\text{Born}}(s) \tag{9}$$

is the Born approximation value for the helicity conserving S-wave multipole. Again in order to compare with data we integrate Eq. (7) to yield

$$\sigma^C(|\cos\theta| < Z) = \frac{\pi\alpha^2\beta(s)}{s}\left[2Z\left(|a|^2 + 2 - 2\,\text{Re}a + \frac{[1 - \beta^2(s)]^2}{1 - \beta^2(s)Z^2}\right) + \frac{1 - \beta^2(s)}{\beta(s)}\ln\left(\frac{1 + \beta(s)Z}{1 - \beta(s)Z}\right)[2\,\text{Re}a - 3 - \beta^2(s)]\right]. \tag{10}$$

In the threshold region the phase of $f_I(s)$ is required by unitarity to be equal to the corresponding $\pi\pi$ phase shift $\delta_I(s)$. When $s > 16m_\pi^2$, inelastic reactions involving four pions are allowed. However, the inelasticity is small, being of order E^8 in the chiral expansion and also sup-

pressed by phase space considerations. In practice, the inelasticity is negligible up to $K\bar{K}$ threshold, $s \sim 1$ GeV^2, and consequently we will neglect inelasticity throughout our analysis.

The functions $f_I(s)$ are then analytic functions of s

except for cuts along the positive and negative real axis. For positive s, the right-hand cut extends from $4m_\pi^2 < s < \infty$ and is due to the s-channel $\pi\pi$ state. For negative s, the left-hand cut is due to t-, u-channel intermediate states such as $\gamma\pi \to \pi \to \gamma\pi$ or $\gamma\pi \to \rho \to \gamma\pi$, and extends from $-\infty < s < 0$.

The single-channel final state unitarization problem has a simple solution in terms of the Omnes function [11]:

$$D_I^{-1}(s) = \exp\left(\frac{s}{\pi}\int_{4m_\pi^2}^{\infty}\frac{ds'}{s'}\frac{\delta_I(s')}{s'-s-i\epsilon}\right). \quad (11)$$

The result must have the form

$$f_I(s) = g_I(s)D_I^{-1}(s), \quad (12)$$

where $g_I(s)$ is an analytic function with no cuts along the positive real axis. Morgan and Pennington consider a function $p_I(s)$ which has the same left-hand singularity structure as $f_I(s)$, but which is real for $s > 0$. They then write a twice subtracted dispersion relation for the difference $[f_I(s) - p_I(s)]D_I(s)$, with the result [7]

$$f_I(s) = D_I^{-1}(s)\left[p_I(s)D_I(s) + (c_I + sd_I)\right.$$
$$\left. -\frac{s^2}{\pi}\int_{4m_\pi^2}^{\infty}\frac{ds'}{s'^2}\frac{p_I(s')\mathrm{Im}D_I(s')}{s'-s-i\epsilon}\right], \quad (13)$$

where c_I, d_I are subtraction constants. The combination inside the square brackets is real with any $p_I(s)$ which is real for $s > 0$. By Low's theorem f_I must reduce to the Born term at low energies [12],

$$f_I(s) = f_I^{\mathrm{Born}}(s) + O(s) = p_I(s) + c_I + d_I s + \cdots, \quad (14)$$

so that we can set $c_I = 0$ if we choose $p_I(s) = f_I^{\mathrm{Born}} + O(s)$. The only assumption made thus far has been the neglect of inelastic channels.

Analyticity and unitarity do *not* determine the remaining subtraction constants d_0, d_2. However, by matching the dispersion relation with the low-energy chiral representation one can express d_0, d_2 in terms of known chiral low-energy constants. This methodology was developed in Ref. [13], and we apply it here. At low energies we set

$$p_I(s) = f_I^{\mathrm{Born}}(s), \qquad \mathrm{Im}D_I(s) = -\beta(s)t_I^{\mathrm{CA}}(s), \quad (15)$$

where $t_I^{\mathrm{CA}}(s)$ are the lowest-order (Weinberg) $\pi\pi$ scattering amplitudes [14]

$$t_0^{\mathrm{CA}}(s) = \frac{2s - m_\pi^2}{32\pi F_\pi^2}, \qquad t_2^{\mathrm{CA}}(s) = -\frac{s - 2m_\pi^2}{32\pi F_\pi^2}. \quad (16)$$

Since these are simple polynomials of the form $t_I^{\mathrm{CA}}(s) = a + bs$, the dispersive integral can be evaluated exactly[2]

$$-\frac{s^2}{\pi}\int_{4m_\pi^2}^{\infty}\frac{ds'}{s'^2}\frac{1-\beta^2(s')}{2\beta(s')}\ln\left(\frac{1+\beta(s')}{1-\beta(s')}\right)\frac{\beta(s')t_I^{\mathrm{CA}}(s')}{s'-s-i\epsilon} = \frac{1-\beta^2(s)}{4\pi}\ln^2\left(\frac{\beta(s)+1}{\beta(s)-1}\right)t_I^{\mathrm{CA}}(s) + \frac{1}{\pi}t_I^{\mathrm{CA}}(s) + \frac{s}{12\pi m_\pi^2}t_I^{\mathrm{CA}}(0) \quad (17)$$

which yields a representation for the scattering amplitude [15]

$$f_I(s) \equiv f_I^{\mathrm{Born}}(s) + g_I(s)$$
$$= D_I^{-1}(s)\left[D_I(s)\frac{1-\beta^2(s)}{2\beta(s)}\ln\left(\frac{1+\beta(s)}{1-\beta(s)}\right) - \frac{1}{4\pi}[1-\beta^2(s)]t_I^{\mathrm{CA}}(s)\ln^2\left(\frac{\beta(s)+1}{\beta(s)-1}\right)\right.$$
$$\left. -\frac{1}{\pi}t_I^{\mathrm{CA}}(s) + s\left(d_I - \frac{t_I^{\mathrm{CA}}(0)}{12\pi m_\pi^2}\right) + \Delta_I(s)\right]. \quad (18)$$

Here $\Delta_I(s)$ represents the remainder which accounts for the difference in the true dispersion integral from the lowest-order inputs given in Eq. (15). At low energies $\Delta_I(s) \sim O(s^2)$. Equation (18) can be compared with the one-loop $O(E^4)$ chiral amplitude which has the form [4]

$$f_I^{\mathrm{Chiral}}(s) = \frac{1-\beta^2(s)}{2\beta(s)}\ln\left(\frac{1+\beta(s)}{1-\beta(s)}\right)$$
$$-\frac{1-\beta^2(s)}{4\pi}t_I^{\mathrm{CA}}(s)\ln^2\left(\frac{\beta(s)+1}{\beta(s)-1}\right)$$
$$-\frac{1}{\pi}t_I^{\mathrm{CA}}(s) + \frac{2}{F_\pi^2}(L_9^r + L_{10}^r)s + \cdots, \quad (19)$$

where $L_9^r + L_{10}^r$ is a combination of known chiral low-energy constants. This combination is independent of

the renormalization scale and has magnitude [16]

$$L_9^r + L_{10}^r = (1.43 \pm 0.27) \times 10^{-3} \quad (20)$$

determined from radiative pion decay. Thus chiral symmetry fixes unambiguously the subtraction constants which appear in the dispersive analysis:

$$d_I = \frac{2}{F_\pi^2}(L_9^r + L_{10}^r) + \frac{t_I^{\mathrm{CA}}(0)}{12\pi m_\pi^2}. \quad (21)$$

---

[2]Note that both left- and right-hand sides of this equation have identical imaginary parts and behave as $O(s^2)$ for $s \sim 0$.

The two formalisms match very nicely at low energy yielding a parameter-free descriptive of the low-energy $\gamma\gamma \to \pi\pi$ process.

At this stage we can inquire into the origin of the large corrections found in the $\gamma\gamma \to \pi^0\pi^0$ amplitude. Do they arise simply from the unitarization of the amplitude [i.e., $D_I(s) \neq 1$] or are new inputs needed in the amplitude [in which case $\Delta_I(s)$ would be most important]? We will argue that the rescattering physics in $D_I^{-1}(s)$ is most important, and that the main corrections are due to well-known ingredients. In the next section, we will attempt a full phenomenological treatment but here let us explore the case with $\Delta_I(s) = 0$ and a simple analytic form for $D_I^{-1}(s)$. The condition $\mathrm{Im}D_I(s) = -\beta t_I^{CA}(s)$ defines the [0,1] Padé approximation for the Omnes function [16], i.e.,

$$D_I^{-1}(s) = \frac{1}{1 - k_I s + t_I^{CA}(s)[h(s) - h(0)]}$$

with

$$h(s) = \frac{\beta(s)}{\pi} \ln\left(\frac{\beta(s)+1}{\beta(s)-1}\right), \qquad h(0) = \frac{2}{\pi} \qquad (22)$$

and allows one an approximate but simple analytic representation for the $\gamma\gamma \to \pi\pi$ amplitude, so we will use this form in the remainder of this section. The constant $k_0 \cong \frac{1}{25m_\pi^2}$ is chosen to match the small s behavior of the experimental $D_0^{-1}(s)$ function, and $k_2 \cong -\frac{1}{30m_\pi^2}$ is chosen from a fit to $I = 2$ $\pi\pi$ scattering. For more details of both of these ingredients, see Sec. III. The resulting form for the $\gamma\gamma \to \pi^0\pi^0$ amplitude is

$$f^N(s) = -\frac{1}{48\pi^2 F_\pi^2}\left[1 + \frac{m_\pi^2}{s}\ln^2\left(\frac{\beta(s)+1}{\beta(s)-1}\right)\right]$$
$$\times\left[(2s - m_\pi^2)D_0^{-1}(s) + (s - 2m_\pi^2)D_2^{-1}(s)\right]$$
$$+\frac{4}{3F_\pi^2}(L_9^r + L_{10}^r)s[D_0^{-1}(s) - D_2^{-1}(s)] \qquad (23)$$

which, when the Padé forms of $D_I^{-1}(s)$ are used, provides a consistent analytic solution to the dispersion relation while also displaying the correct chiral properties to $O(s)$. In Fig. 3, we plot the resulting cross section, in comparison with the data and the lowest-order result. It can be seen that the Omnes functions produce a substantial modification even near threshold. Of these, the more important is $D_0^{-1}(s)$ which reflects the strong attractive $\pi\pi$ scattering in the $I = 0, J = 0$ channel [17,18]. The use of an empirical determination of $D_0^{-1}(s)$ in the next section will further increase the amplitude. While refinements can be added to the calculation of the amplitude, we conclude that the major ingredient which modifies the threshold behavior in $\gamma\gamma \to \pi^0\pi^0$ is the final state rescattering corrections.

That such corrections might be important is perhaps in retrospect not so surprising. Chiral perturbation theory represents an expansion in energy with a scale of order $\Lambda_\chi \sim 4\pi F_\pi \sim 1$ GeV [19]. For center-of-mass energies $\sqrt{s} \leq 0.5$ GeV one would expect that χPT should give an accurate representation of the scattering amplitude,
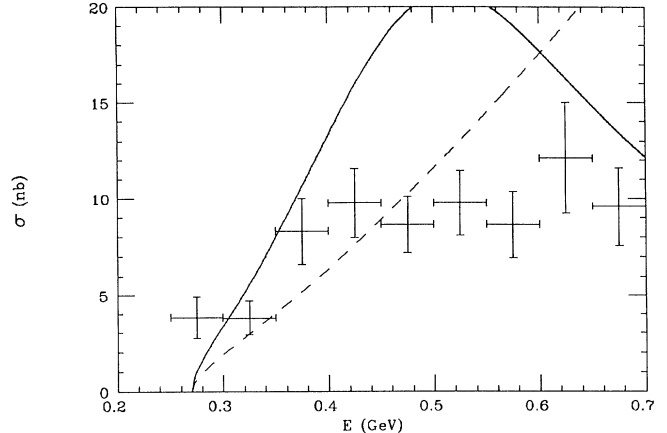

FIG. 3. Shown is the $\gamma\gamma \to \pi^0\pi^0$ cross section predicted by one-loop chiral perturbation theory (dashed line) and by the simple analytic Padé solution to the dispersion relations (solid line).

and this is indeed the case for the $\gamma\gamma \to \pi^+\pi^-$ process. However, for $\gamma\gamma \to \pi^0\pi^0$ there exist no Born or $O(E^4)$ counterterm contributions. The $O(E^4)$ amplitude arises entirely from one-loop effects and is consequently nearly an order of magnitude smaller than its charged pion counterpart. It is this smallness which accounts for the importance of higher-order effects, and one should be alerted to the possible significance of such corrections in other such processes such as $K_S \to 2\gamma, K_L \to \pi^0\gamma\gamma, \eta^0 \to \pi^0\gamma\gamma$, etc.

III. FURTHER REFINEMENT

The analysis of the previous section was done in a particularly naive limit in order to expose the essential physics in the clearest fashion. Although this provides a good description of the threshold region, in phenomenological studies one may be interested in a more complete calculation. We provide this in the present section. In particular we add the following ingredients.

(i) The Omnes function $D_0^{-1}(s)$ has been determined from the experimental phase shifts by Donoghue et al. [13]. We use this in place of the Padé approximation Eq. (22).

(ii) The Born amplitude is not sufficient to fully describe the $\gamma\gamma\pi\pi$ vertex which receives further contributions from $\rho, \omega, A1$ exchanges. We add these to the formalism. The resulting amplitude is similar to that of Morgan and Pennington [9] with the exception of the related ingredients of $L_9^r + L_{10}^r$ and $A1$ exchange. As we describe more fully below, the $A1$ contribution is in fact more important at low energy than is the effect of the ρ and ω.

The Omnes function involves an integral over the $\pi\pi$ scattering phase shifts. These are known experimentally up to above 1 GeV, and at low s the Omnes function is not very sensitive to the phase shifts beyond their known range. Donoghue et al. have taken this data, added chiral constraints at low energy where the data is somewhat

poor, and performed a numerical evaluation of $D_0^{-1}(s)$ [20]. The result is somewhat larger in both the real and imaginary parts than the Padé approximation used in the last section. The form of the $I = 2$ Omnes function is not as important because $D_2^{-1}(s)$ remains closer to unity. In this case we use the Padé form, given in Eq. (22). The constant k_2 is chosen so that the $\pi\pi$ scattering amplitude, defined by

$$t_2(s) = t_2^{CA}(s)D_2^{-1}(s),\qquad(24)$$

matches the experimental phase shifts over the region $4m_\pi^2 \leq s \leq 1$ GeV^2. We find that the constant $k_2 = -\frac{1}{30m_\pi^2}$ provides a good fit throughout this region. We note that Gasser and Meissner compare the $I = 0$ Padé approximation with the full Omnes function and with a

two-loop chiral calculation and find that the Padé form does not completely characterize the chiral logarithms properly [21]. While it is important to keep in mind that the Padé procedure is only an approximation, the numerical differences are not large if the free parameter is chosen properly. We expect that in the $I = 2$ channel the Padé form should be numerically a good approximation. Use of these result in the dispersive formula of Eq. (13), with $p_I(s) = f_I^{\text{Born}}(s)$, yields the curve in Fig. 4.

The $\gamma\pi \to \gamma\pi$ Compton amplitude receives important modification at low energy from ρ and the $A1$ exchange, as shown in Fig. 5. These have been analyzed in detail in Ref. [22]. In particular, the Compton amplitude including these poles in a vector dominance model is given by

$$\frac{1}{4\pi\alpha}T_{\mu\nu}(p_1,q_1,q_2) = 2g_{\mu\nu} - \frac{T_\mu(p_1,p_1+q_1)T_\nu(p_2+q_2,p_2)}{(p_1+q_1)^2-m_\pi^2} - \frac{T_\nu(p_1,p_1-q_2)T_\mu(p_2-q_1,p_2)}{(p_1-q_2)^2-m_\pi^2}$$

$$+\frac{F_V^2}{F_\pi^2}\left[g_{\mu\nu}\left(\frac{q_2^2}{m_V^2-q_2^2}+\frac{q_1^2}{m_V^2-q_1^2}\right)-q_{1\mu}q_{1\nu}\frac{1}{m_V^2-q_1^2}-q_{2\mu}q_{2\nu}\frac{1}{m_V^2-q_2^2}\right]$$

$$-\frac{F_A^2}{F_\pi^2}(g_{\mu\nu}q_1\cdot q_2-q_{1\nu}q_{2\mu})\left[\frac{1-\frac{p_1\cdot(p_1+q_1)}{m_A^2}}{m_A^2-(p_1+q_1)^2}+\frac{1-\frac{p_1\cdot(p_1-q_2)}{m_A^2}}{m_A^2-(p_1-q_2)^2}\right]$$

with

$$T_\mu(p_1,p_2) = (p_1+p_2)_\mu + \frac{F_V^2}{2F_\pi^2(m_V^2-q^2)}\left[(p_1+p_2)_\mu q^2-(p_1-p_2)_\mu(p_1^2-p_2^2)\right].\qquad(25)$$

This is to be compared with the chiral form of the amplitude

$$\frac{1}{4\pi\alpha}T_{\mu\nu}(p_1,q_1,q_2) = 2g_{\mu\nu} - \frac{T_\mu(p_1,P_1+q_1)T_\nu(p_2+q_2,p_2)}{(p_1+q_1)^2-m_\pi^2} - \frac{T_\nu(p_1,p_1-q_2)T_\mu(p_2-q_1,p_2)}{(p_1-q_2)^2-m_\pi^2}$$

$$+\frac{4}{F_\pi^2}L_9^r[(q_1^2+q_2^2)g_{\mu\nu}-q_{1\mu}q_{1\nu}-q_{2\mu}q_{2\nu}]-\frac{8}{F_\pi^2}(L_9^r+L_{10}^r)(q_1\cdot q_2g_{\mu\nu}-q_{2\nu}q_{1\nu})$$

with

$$T_\mu(p_1,p_2) = (p_1+p_2)_\mu\left(1+\frac{2L_9^r}{F_\pi^2}q^2\right)-(p_1-p_2)_\mu\frac{2L_9^r}{F_\pi^2}(p_1^2-p_2^2).\qquad(26)$$

We see from this that this parameter L_9^r is due to ρ exchange, L_{10}^r involves $\rho + A1$ while the combination $L_9^r + L_{10}^r$ is purely $A1$ exchange if the Kawarabayashi-Suzuki-Fayyazuddin-Riazuddin (KSFR) relation, $m_A = \sqrt{2}m_\rho$, is used [23]. These features are by now well known. Thus the lowest-order form of these has already been included in the previous analysis through the constant $L_9^r + L_{10}^r$. However, as the energy is increased the momentum dependence in the propagator becomes more important and should be explicitly included. There is also the effect of ρ and ω exchanges from Fig. 6. The $\rho\pi\gamma$ and $\omega\pi\gamma$ couplings are of the form

$$A(V \to \pi\gamma) = \frac{1}{2}\sqrt{R_V}\epsilon^{\mu\nu\alpha\beta}V_{\mu\nu}\epsilon_\alpha p_{\pi\beta}.\qquad(27)$$

Because of the powers of momentum in the vertex, the effect of these diagrams are suppressed at low energy, being of order E^6 in the chiral expansion. It is interesting that $A1$ exchange is more important than ρ and ω at low energies, and this point has been overlooked in Ref. [9].
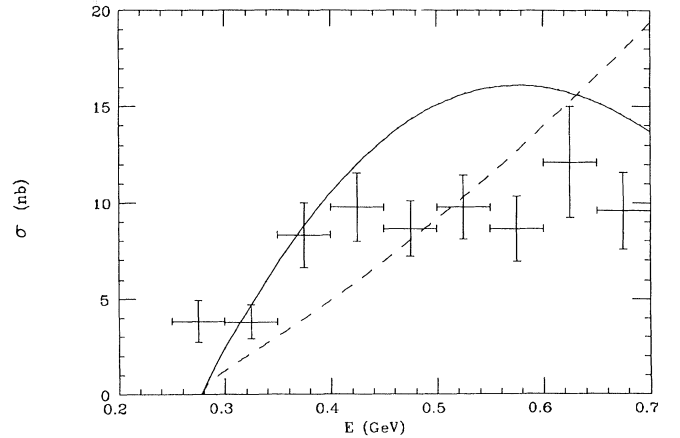

FIG. 4. Shown is the $\gamma\gamma \to \pi^0\pi^0$ cross section predicted by one-loop chiral perturbation theory (dashed line) and by a dispersive treatment using an Omnes function generated from experimental $\pi\pi$ phase shifts in the S-wave $I = 0$ channel (solid line).
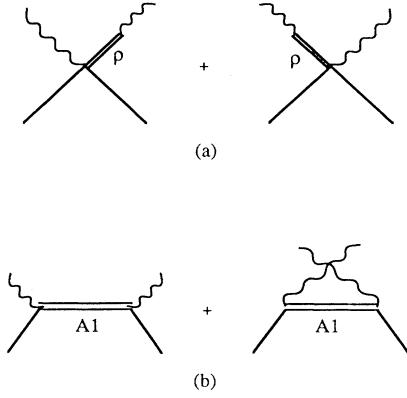
(a)

(b)

FIG. 5. Shown are ρ and $A1$ exchange diagrams which affect the Compton scattering amplitude at $O(p^4)$.

Thus the S-wave projections to be used in the dispersive integral should be [24]

$$p_I(s) = f_I^{\text{Born}}(s) + p_{AI}(s) + p_{\rho I}(s) + p_{\omega I}(s),$$

$$p_{A0} = p_{A2}$$
$$= \frac{(L_9^r + L_{10}^r)}{F_\pi^2}\left[\frac{m_A^2 - m_\pi^2}{\beta(s)}\ln\left(\frac{1+\beta(s)+\frac{s_A}{s}}{1-\beta(s)+\frac{s_A}{s}}\right) + s\right],$$

$$p_{\rho 0} = -\frac{3R_\rho}{2}\left[\frac{m_\rho^2}{\beta(s)}\ln\left(\frac{1+\beta(s)+\frac{s_\rho}{s}}{1-\beta(s)+\frac{s_\rho}{s}}\right) - s\right], \quad (28)$$

$$p_{\rho 2} = 0,$$

$$p_{\omega 0} = -\frac{1}{2}p_{\omega 2} = -\frac{R_\omega}{2}\left[\frac{m_\omega^2}{\beta(s)}\ln\left(\frac{1+\beta(s)+\frac{s_\omega}{s}}{1-\beta(s)+\frac{s_\omega}{s}}\right) - s\right],$$

where $s_i = 2(m_i^2 - m_\pi^2)$ and $R_\omega = 1.35$ GeV^{-2}, $R_\rho = 0.12$ GeV^{-2} are determined from the condition
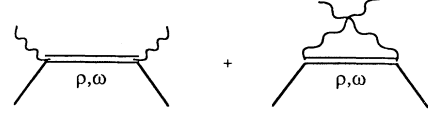

FIG. 6. Shown are ρ and ω exchange diagrams which affect the Compton scattering amplitude at $O(p^6)$.

$$R_V = \frac{6m_V^3}{\alpha}\frac{\Gamma(V \to \pi\gamma)}{(m_V^2 - m_\pi^2)^3}. \quad (29)$$

The connection with our previous formalism may be found by taking the limit $s \to 0$, whereby we find

$$\lim_{s\to 0} p_{A0}(s) = \lim_{s\to 0} p_{A2}(s) = \frac{2(L_9^r + L_{10}^r)}{F_\pi^2}s,$$

$$\lim_{s\to 0} p_{\rho 0}(s) = O(s^2), \quad (30)$$

$$\lim_{s\to 0} p_{\omega 0}(s) = -\frac{1}{2}\lim_{s\to 0} p_{\omega 2}(s) = O(s^2).$$

We observe that the contribution from ω, ρ exchange is $O(s^2)$ and is outside the original chiral expansion, as claimed, while that from $A1$ exchange accounts for the $O(s)$ chiral contribution from $L_9 + L_{10}$. Thus since this piece is automatically included in the $A1$ exchange term, we must modify the associated subtraction constants to become

$$d_I = \frac{t_I^{\text{CA}}(0)}{12\pi m_\pi^2}. \quad (31)$$

The contribution of the vector meson exchange terms can then be included by defining the general Compton scattering amplitude as [24]

$$\frac{1}{16\pi\alpha}T_{\mu\nu}(p_1, q_1, q_2) \equiv A(q_{2\mu}q_{1\nu} - q_1\cdot q_2 g_{\mu\nu}) + B\left(\frac{p_1\cdot q_1 p_1\cdot q_2}{q_1\cdot q_2}g_{\mu\nu} + p_{1\mu}p_{1\nu} - \frac{p_1\cdot q_1}{q_1\cdot q_2}q_{2\mu}p_{1\nu} - \frac{p_1\cdot q_2}{q_1\cdot q_2}q_{1\nu}p_{1\mu}\right). \quad (32)$$

The neutral pion production cross section then can be written as

$$\gamma\gamma \to \pi^0\pi^0 : \quad \sigma^N(|\cos\theta| < Z) = \frac{\pi\alpha^2}{s^2}\int_{t_a}^{t_b} dt\left(|A^0 s - m_\pi^2 B^0|^2 + \frac{|B^0|^2}{s^2}(m_\pi^4 - tu)\right), \quad (33)$$

where

$$t_{\substack{b\\a}} = m_\pi^2 - \frac{1}{2}s \pm \frac{sZ}{2}\beta(s) \quad (34)$$

and

$$sA^0 = -\frac{2}{3}[f_0(s) - f_2(s)] + \frac{2}{3}[p_0(s) - p_2(s)] - \frac{s}{2}\sum_{V=\rho,\omega} R_V\left(\frac{m_\pi^2 + t}{t - m_V^2} + \frac{m_\pi^2 + u}{u - m_V^2}\right),$$

$$(35)$$

$$B^0 = -\frac{s}{2}\sum_{V=\rho,\omega} R_V\left(\frac{1}{t - m_V^2} + \frac{1}{u - m_V^2}\right),$$

while for charged pion production

$$\gamma\gamma \to \pi^+\pi^- : \quad \sigma^C(|\cos\theta| < Z) = \frac{2\pi\alpha^2}{s^2} \int_{t_a}^{t_b} dt \left(|A^+ s - m_\pi^2 B^+|^2 + \frac{|B^+|^2}{s^2}(m_\pi^4 - tu) \right) \tag{36}$$

with

$$sA^+ = -\frac{1}{3}[2f_0(s) + f_2(s)] + \frac{1}{3}[2p_0(s) + p_2(s)]$$

$$-\frac{s}{2}R_\rho \left(\frac{m_\pi^2 + t}{t - m_\rho^2} + \frac{m_\pi^2 + u}{u - m_\rho^2} \right)$$

$$+m_A^2 s \frac{L_9^r + L_{10}^r}{F_\pi^2} \left(\frac{1 - \frac{m_\pi^2 + t}{2m_A^2}}{t - m_A^2} + \frac{1 - \frac{m_\pi^2 + u}{2m_A^2}}{u - m_A^2} \right),$$

$$\tag{37}$$

$$B^+ = -\left(\frac{1}{t - m_\pi^2} + \frac{1}{u - m_\pi^2} \right)$$

$$-\frac{sR_\rho}{2} \left(\frac{1}{t - m_\rho^2} + \frac{1}{u - m_\rho^2} \right).$$

Note that here the functions f_I employ the modified subtraction constant Eq. (28) and that the dispersion integrals utilize the full function $p_I(s)$ defined in Eq. (26). The integration over t is performed analytically while the dispersive integration is done numerically. This then is our final form and yields results for neutral and charged pion production as shown in Figs. 2 and 7. Note that in the low-energy region *both* cross sections are in good agreement with the experimental data. We should not expect consistency in the higher-energy sector—$\sqrt{s} \geq$ 700 MeV—as important resonant effects associated with the $f_0(975), f_2(1270)$ have not been included [25].
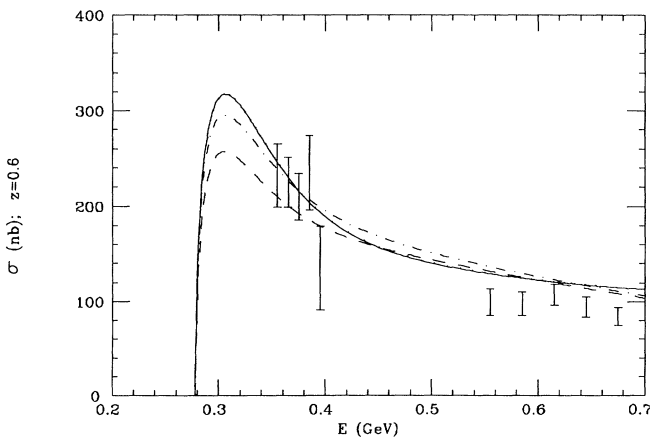

FIG. 7. Shown is the $\gamma\gamma \to \pi^+\pi^-$ cross section predicted by the Born approximation (dashed line), by one-loop chiral perturbation theory (dot-dashed line), and by a full dispersive treatment as described in the text (solid line).

IV. PION POLARIZABILITY

The electromagnetic polarizability is a fundamental property of an elementary particle which measures its deformation in the presence of an external electric-magnetic field [26]. In the case of an atomic system this property can be probed by detection of the effects induced by the interaction of an electromagnetic signal with a "box" filled with such atoms. An example is provided by the recent measurements of the proton polarizability as a byproduct of low-energy Compton scattering measurements on a hydrogen target. In the case of the pion, of course, an appropriate target is not available. Nevertheless, it is possible to probe the pion polarizability by measuring the Compton scattering amplitude, just as in the nucleonic analog, by exploiting either the process of radiative pion-nucleon scattering $\pi N \to \pi N\gamma$ [Fig. 8(a)], pion photoproduction in photon-nucleon scattering $\gamma N \to \gamma N\pi$ [Fig. 8(b)] or direct $\gamma\gamma \to \pi\pi$ measurements [Fig. 8(c)]. None of these experiments is straightforward. However, in the case of the charged pion each has been used to measure the polarizability, yielding somewhat discrepant results:

$$\begin{align}
\text{(a)} \quad & \bar{\alpha}_E^{\pi^+} = (6.8 \pm 1.4 \pm 1.2) \times 10^{-4} \text{ fm}^3, \\
\text{(b)} \quad & \bar{\alpha}_E^{\pi^+} = (20 \pm 12) \times 10^{-4} \text{ fm}^3, \tag{38} \\
\text{(c)} \quad & \bar{\alpha}_E^{\pi^+} = (2.2 \pm 1.6) \times 10^{-4} \text{ fm}^3
\end{align}$$

(Refs. [27–29], respectively). For neutral pions, only the $\gamma\gamma \to \pi\pi$ reaction has been employed, and separate analysis using very different assumptions have yielded the results

$$\text{(d)} \quad |\bar{\alpha}_E^{\pi^+}| = (0.69 \pm 0.07 \pm 0.04) \times 10^{-4} \text{ fm}^3,$$

$$\tag{39}$$

$$\text{(e)} \quad |\bar{\alpha}_E^{\pi^+}| = (0.8 \pm 2.0) \times 10^{-4} \text{ fm}^3$$

(Refs. [29,30], respectively). Such measurements are of particular interest in that, as we shall show, for both charged and neutral pions chiral symmetry makes what should be a very reliable prediction for the size of the polarizability [31],

$$\bar{\alpha}_E^{\pi^+} = 2.7 \times 10^{-4} \text{ fm}^3,$$

$$\tag{40}$$

$$\bar{\alpha}_E^{\pi^0} = -0.5 \times 10^{-4} \text{ fm}^3,$$

and thus the possible discrepancies indicated by the data are potentially very significant.

In this section we examine the $\gamma\gamma \to \pi\pi$ process as a probe of the polarizability. In particular we have seen that dispersion relations coupled with chiral perturbation theory can be used in order to obtain a very ac-

curate description of the $\gamma\gamma \to \pi\pi$ cross section in the region $\sqrt{s} < 1$ GeV and this analysis can be modified in order to provide an experimental measure of the polarizability. The connection of the Compton amplitude with the polarizability may be found by noting that for a particle with electric-magnetic polarizability α_E/β_M the associated energy is

$$U = -\frac{1}{2}4\pi\bar{\alpha}_E\mathbf{E}^2 - \frac{1}{2}4\pi\bar{\beta}_M\mathbf{H}^2. \tag{41}$$

Since, using our choice of gauge $\mathbf{E} \sim -i\omega\hat{\epsilon}$, $\mathbf{B} = i\mathbf{k}\times\hat{\epsilon}$ we can identify the polarizability in terms of the low-energy (cross channel) Compton scattering amplitude via

$$\text{Amp} = \hat{\epsilon}_1 \cdot \hat{\epsilon}_2 \left(-\frac{\alpha}{m_\pi} + 4\pi\bar{\alpha}_E\omega_1\omega_2\right)$$

$$+\hat{\epsilon}_1 \times \mathbf{k}_1 \cdot \hat{\epsilon}_2 \times \mathbf{k}_24\pi\bar{\beta}_M + \cdots. \tag{42}$$

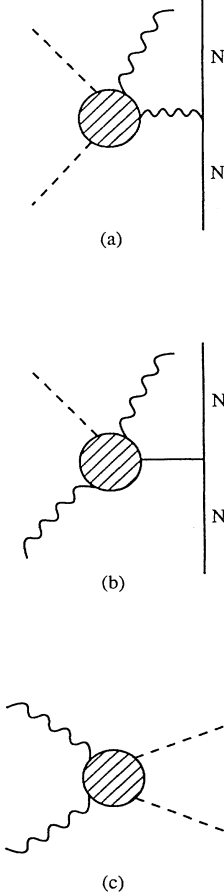We find then [32]

(a)

(b)

(c)

FIG. 8. Indicated are the various ways of obtaining experimental values for the pion polarizability: (a) radiative pion-nucleon scattering, (b) pion photoproduction in photon-nucleon scattering, and (c) direct $\gamma\gamma \to \pi\pi$ measurements.

$$\bar{\alpha}_E^{\pi^+} = -\lim_{t\to m_\pi^2, s\to 0} \frac{2\alpha}{m_\pi}\left(A^+(s,t) + \frac{t-3m_\pi^2}{s}\tilde{B}^+(s,t)\right)$$

$$= 2.68 \times 10^{-4} \text{ fm}^3, \tag{43}$$

$$\bar{\beta}_M^{\pi^+} = \lim_{t\to m_\pi^2, s\to 0} \frac{2\alpha}{m_\pi}\left(A^+(s,t) + \frac{t-m_\pi^2}{s}\tilde{B}^+(s,t)\right)$$

$$= -2.61 \times 10^{-4} \text{ fm}^3,$$

$$\bar{\alpha}_E^{\pi^0} = -\lim_{t\to m_\pi^2, s\to 0} \frac{2\alpha}{m_\pi}\left(A^0(s,t) + \frac{t-3m_\pi^2}{s}B^0(s,t)\right)$$

$$= -0.50 \times 10^{-4} \text{ fm}^3,$$

$$\bar{\beta}_M^{\pi^0} = \lim_{t\to m_\pi^2, s\to 0} \frac{2\alpha}{m_\pi}\left(A^0(s,t) + \frac{t-m_\pi^2}{s}B^0(s,t)\right)$$

$$= 1.26 \times 10^{-4} \text{ fm}^3,$$

where we have defined

$$\tilde{B}^+(s,t) \equiv B^+(s,t) - B_{\text{Born}}^+(s,t). \tag{44}$$

Note that these forms do not obey the conventional stricture $\bar{\alpha}_E^\pi = -\bar{\beta}_M^\pi$ which is obtained in the chiral limit [33]. However, this condition *is* satisfied if we take $m_\pi \to 0$ as can be seen from the relations [32]

$$\bar{\alpha}_E^{\pi^+} + \bar{\beta}_M^{\pi^+} = 4\alpha m_\pi\frac{R_\rho}{m_\rho^2 - m_\pi^2}$$

$$\approx 0.064\{0.39 \pm 0.04\} \times 10^{-4} \text{ fm}^3, \tag{45}$$

$$\bar{\alpha}_E^{\pi^0} + \bar{\beta}_M^{\pi^0} = 4\alpha m_\pi\sum_V\frac{R_V}{m_V^2 - m_\pi^2}$$

$$\approx 0.76\{1.04 \pm 0.07\} \times 10^{-4} \text{ fm}^3.$$

Thus the violations of this condition arise from the vector meson exchange contributions, which are $O(E^6)$ in the chiral expansion [1]. It is also interesting to see that both of the equations (45) are positive in agreement with the dispersion relation requirement

$$\bar{\alpha}_E + \bar{\beta}_M = \frac{1}{2\pi^2}\int_0^\infty \frac{d\omega\sigma_{\text{tot}}(\omega)}{\omega^2}, \tag{46}$$

experimental evaluation of which gives the bracketed values indicated in Eq. (45) [9]. In terms of these definitions the $\gamma\gamma \to \pi\pi$ amplitudes can be parametrized as

$$f_{\pi^+}(s) = \frac{1-\beta^2(s)}{2\beta(s)}\ln\left(\frac{1+\beta(s)}{1-\beta(s)}\right)$$

$$+\frac{m_\pi}{4\alpha}(\bar{\alpha}_E^{\pi^+} - \bar{\beta}_M^{\pi^+})s + O(s^2, sm_\pi^2), \tag{47}$$

$$f_{\pi^0}(s) = \frac{m_\pi}{4\alpha}(\bar{\alpha}_E^{\pi^0} - \bar{\beta}_M^{\pi^0})s + O(s^2, sm_\pi^2),$$

where the explicit form of the $O(s^2)$ terms can be read off from Eq. (13). (Note that in this case, unlike that of Compton scattering, the photons are colinear in the center of mass so that electric and magnetic polarizability terms cannot be separated and always appear in the

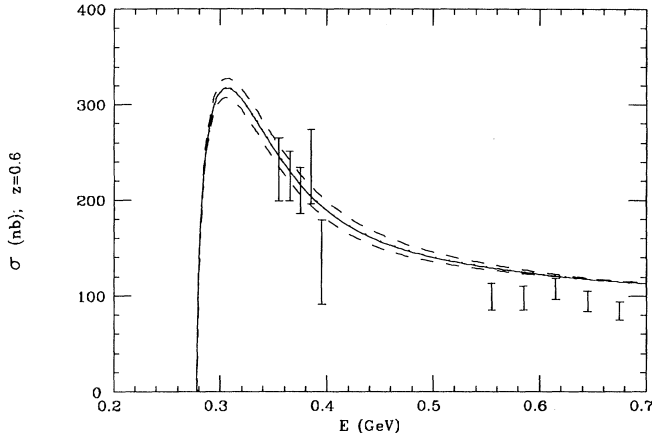PHOTON-PHOTON SCATTERING, PION POLARIZABILITY, ...

FIG. 9. Shown is the $\gamma\gamma \rightarrow \pi^+\pi^-$ cross section predicted by the full dispersive calculation and with $\bar{\alpha}_E^{\pi^+} = 2.8 \times 10^{-4}$ fm^3 (solid line), with $\bar{\alpha}_E^{\pi^+} = 4.2 \times 10^{-4}$ fm^3 (upper dotted line), and with $\bar{\alpha}_E^{\pi^+} = 1.4 \times 10^{-4}$ fm^3 (lower dotted line).

combination $\bar{\alpha}_E - \bar{\beta}_M$.) Then instead of using the chiral symmetry requirements as input we can modify the linear component of the Compton amplitude in order to gauge the sensitivity of the $\gamma\gamma \rightarrow \pi\pi$ as a probe of pion polarizability. Results of such variation are shown in Figs. 9 and 10 for charged and neutral production, respectively.

In the former case, it is clear that the experimental cross section is in good agreement with the chiral symmetry prediction $\bar{\alpha}_E = 2.7 \times 10^{-4}$ fm^3. However, even 100% changes in this value are also consistent with the low-energy data, as is clear from Fig. 9. We conclude that although $\gamma\gamma \rightarrow \pi^+\pi^-$ measurements certainly have the potential to provide a precise value for the pion polarizability, the statistical uncertainty of the present values does not allow a particularly precise evaluation. In this
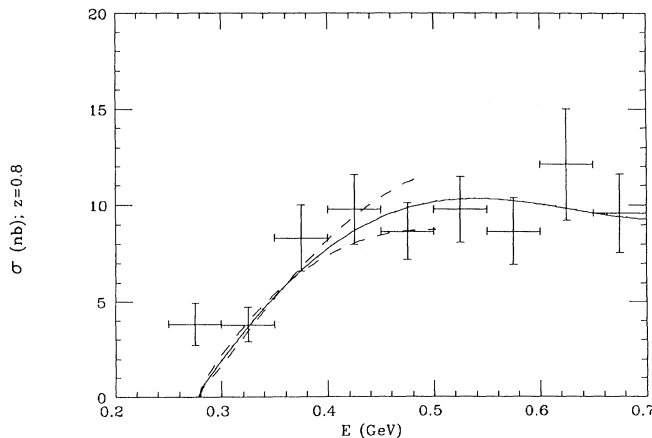

FIG. 10. Shown is the $\gamma\gamma \rightarrow \pi^0\pi^0$ cross section predicted by the full dispersive calculation and with $\bar{\alpha}_E^{\pi^0} = -0.5 \times 10^{-4}$ fm^3 (solid line), with $\bar{\alpha}_E^{\pi^0} = -1.3 \times 10^{-4}$ fm^3 (upper dotted line), and with $\bar{\alpha}_E^{\pi^0} = +0.3 \times 10^{-4}$ fm^3 (lower dotted line).

regard our conclusions are in agreement with those derived from the one-loop chiral amplitude, although the uncertainty in $\bar{\alpha}_E^{\pi^+}$ quoted by Babusci et al. in Ref. [9] seems somewhat smaller than that indicated in our analysis. Both results, however, appear to be inconsistent with the value $(6.8 \pm 1.4 \pm 1.2) \times 10^{-4}$ fm^3 quoted in Ref. [27].

In the case of neutral pion production our predicted cross section is also in good agreement with the low-energy data and therefore also with the chiral prediction for $\bar{\alpha}_E^{\pi^0}$. However, as shown in Fig. 10 there is very little sensitivity to the polarizability and even much improved measurements will not change this situation. In this regard our conclusions are in strong disagreement with those of Babusci et al. [9] wherein the one loop chiral analysis was used in order to produce a rather precise value for the neutral polarizability: $|\bar{\alpha}_E^{\pi^0}| = 0.69 \pm 0.07 \pm 0.04 \times 10^{-4}$ fm^3. This is because, as shown above, higher loop corrections to the one-loop chiral prediction as given by the dispersive analysis make essential corrections to the lowest-order result and bring agreement with the low-energy data without any need to modify any of the input parameters.

V. CONCLUSIONS

Above we have shown how analyticity can be combined with the strictures of chiral symmetry in order to allow a no-free-parameter description of the low-energy ($E < 0.5$ GeV) $\gamma\gamma \rightarrow \pi\pi$ process. Specifically, building on the work of Morgan and Pennington, a doubly subtracted dispersion relation for the helicity-conserving S-wave amplitude, with the subtraction constants determined in terms of known chiral counterterms, augmented by the Born values for other multipoles, has been shown to be in good agreement with experimental data for both the charged—$\gamma\gamma \rightarrow \pi^+\pi^-$—and neutral— $\gamma\gamma \rightarrow \pi^0\pi^0$— channels. We have also shown how these results can be used in order to experimentally determine values for the pion polarizability $\bar{\alpha}_E^{\pi}$. In the case of the charged pion process, wherein the overall shape of the cross section is dominated by the Born contribution, the one-loop chiral correction which determines the polarizability is the leading correction term and additional (multiloop) effects required by analyticity are found to be small. The value of the charged pion polarizability $\bar{\alpha}_E^{\pi^+}$ determined thereby is in good agreement with both the chiral symmetry prediction as well with that determined in an earlier one-loop chiral analysis of the same data. This value disagrees at the three σ level with that found via radiative pion scattering and calls strongly for a remeasurement of the latter process, as currently proposed at Fermilab. In the case of the neutral pion reaction, there exists no Born term and the requirements of analyticity as embodied in the dispersion analysis are found to make a substantial modification to the one-loop chiral prediction, which involves considerable cancellation between $I = 0, 2$ production amplitudes—the full dispersive calculation is considerably larger in the threshold region than is its one-loop

analog. Use of such a one-loop calculation led recently to a published value for the neutral pion polarizability which was about 40% larger than the chiral requirement [29]. However, the authors of this report noted that their result might well change if multiloop contributions were to be included and we have determined that this is indeed the case—a full dispersive calculation including the strictures of chiral symmetry is in good agreement with the measured neutral pion cross section. Indeed, we conclude from our work that there exists no evidence in either $\gamma\gamma \to \pi^+\pi^-$ or $\gamma\gamma \to \pi^0\pi^0$ for violation of the chiral symmetry predictions for the pion polarizability.

ACKNOWLEDGMENTS

[1] J. Gasser and H. Leutwyler, Ann. Phys. (N.Y.) **158**, 142 (1984); Nucl. Phys. **B250**, 465 (1985).

[2] See, e.g., J. Hamilton, in *Strong Interactions and High Energy Physics*, edited by R.G. Moorhouse (Plenum, New York, 1964), p. 281.

[3] Here the data shown are those of the Mark II Collaboration given by J. Boyer *et al.*, Phys. Rev. D **42**, 1350 (1990). We do not use the corresponding Pluto measurements, which appear to have normalization problems.

[4] J. Bijnens and F. Cornet, Nucl. Phys. **B296**, 557 (1988).

[5] J.F. Donoghue, B.R. Holstein, and Y.-C.R. Lin, Phys. Rev. D **37**, 2423 (1988).

[6] Here the data shown are those of the Crystal Ball Collaboration given by H. Marsiske *et al.*, Phys. Rev. D **41**, 3324 (1990).

[7] D. Morgan and M.R. Pennington, Phys. Lett. B **272**, 134 (1991).

[8] S. Weinberg, Physica A **96**, 327 (1970); for a pedagogical description of chiral perturbation theory see J.F. Donoghue, E. Golowich, and B.R. Holstein, *Dynamics of the Standard Model* (Cambridge University Press, Cambridge, England, 1992).

[9] V.A. Petrun'kin, Fiz. Elem. Chastits At. Yadra **12**, 692 (1981) [Sov. J. Part. Nucl. **12**, 278 (1981)]; D. Babusci *et al.*, Phys. Lett. B **277**, 158 (1992); S. Bellucci, in *DAΦNE Physics Handbook*, edited by L. Maiani, G. Pancheri, and N. Paver (INFN, Frascati, 1992), p. 419.

[10] M.R. Pennington, in *DAΦNE Physics Handbook* [9], p. 379.

[11] R. Omnes, Nuovo Cimento **8**, 316 (1958).

[12] F.E. Low, Phys. Rev. **110**, 174 (1960).

[13] J.F. Donoghue, J. Gasser, and H. Leutwyler, Nucl. Phys. **B343**, 341 (1990).

[14] S. Weinberg, Phys. Rev. Lett. **17**, 616 (1966).

[15] This form is similar to that given by R.L. Goble and J.L. Rosner, Phys. Rev. D **5**, 2345 (1972); R.L. Goble, R. Rosenfeld, and J.L. Rosner, *ibid.* **39**, 3264 (1989).

[16] J. Gasser and H. Leutwyler, Nucl. Phys. **B250**, 465 (1985).

[17] T.N. Truong, Phys. Rev. Lett. **61**, 2526 (1988); A. Dobado, M.J. Herrero, and T.N. Truong, Phys. Lett. B **235**, 134 (1990).

[18] U. Meissner, Comments Nucl. Part. Phys. **20**, 119 (1991).

[19] L. Brown and R. Goble, Phys. Rev. D **4**, 723 (1971); A. Manohar and H. Georgi, Nucl. Phys. **B234**, 189 (1984); J.F. Donoghue, E. Golowich, and B.R. Holstein, Phys. Rev. D **30**, 587 (1984).

[20] J. Gasser, in [13].

[21] J. Gasser and U. Meissner, Nucl. Phys. **B357**, 90 (1991).

[22] J.F. Donoghue, B.R. Holstein, and D. Wyler, Phys. Rev. D **47**, 2089 (1993).

[23] K. Kawarabayashi and M. Suzuki, Phys. Rev. Lett. **16**, 255 (1966); X. Riazuddin and X. Fayyazuddin, Phys. Rev. **147**, 1071 (1966).

[24] P. Ko, Phys. Rev. D **41**, 1531 (1990).

[25] D. Morgan and M.R. Pennington, Z. Phys. C **37**, 431 (1990); A.E. Kaloshin and V.V. Serebryakov, *ibid.* **32**, 279 (1986).

[26] B.R. Holstein, Comments Nucl. Part. Phys. **19**, 221 (1990).

[27] Yu. M. Antipov *et al.*, Phys. Lett. **121B**, 445 (1983); Z. Phys. C **26**, 495 (1985).

[28] T.A. Aibergenov *et al.*, Czech. J. Phys. B **36**, 948 (1986).

[29] D. Babusci *et al.*, Phys. Lett. B **277**, 158 (1992).

[30] A.E. Kaloshin and V.V. Serebryakov, Phys. Lett. B **278**, 198 (1992).

[31] B.R. Holstein, Comments Nucl. Part. Phys. **19**, 221 (1990); M.V. Terent'ev, Yad. Fiz. **16**, 289 (1972) [Sov. J. Nucl. Phys. **16**, 162 (1973)].

[32] D. Babusci *et al.*, DAΦNE Report No. LNF-92/071, 1992 (unpublished).

[33] J.F. Donoghue and B.R. Holstein, Phys. Rev. D **40**, 2378 (1989).